Model quantum magnet. II. Calculation of NMR line shapes

Varsha Banerjee[1,*] and Sushanta Dattagupta[2,†]
[1]*Department of Physics, Indian Institute of Technology, Hauz Khas, New Delhi, 110016, India*
[2]*S. N. Bose National Centre for Basic Sciences, J. D. Block, Salt Lake Sector III, Calcutta, 700098, India*
(Received 26 February 2002; published 16 August 2002)

Following an earlier lead in which we had demonstrated the role of the hyperfine interaction in both the phase diagram and the dynamic susceptibility for a model quantum magnet such as $LiHoF_4$, we calculate the NMR line shape in this system. Although the nuclear quadrupolar component of the interaction is tiny compared to the strength of the (dipolar) hyperfine interaction, the former turns out to be a crucial diagnostic tool, especially near the quantum critical point. We have carried out both a stochastic treatment and an *ab initio* many-body calculation in order to have complementary insight into the algebraic expressions as well as the computed NMR spectra. We hope our derived results will motivate NMR experiments on the quantum critical phenomena in $LiHoF_4$.

DOI: 10.1103/PhysRevB.66.064418 PACS number(s): 75.10.Dg, 76.90.+d

I. INTRODUCTION

In an earlier publication (hereafter referred to as I) we discussed in detail a rare-earth alloy $LiHoF_4$ and argued why this system, in the presence of a transverse magnetic field applied at right angles to the crystalline *c* axis, can be viewed as a quantum magnet.[1] The magnetic properties emanate from a dipolar interaction between the holmium moments which, in the presence of a large uniaxial crystal field term, can be truncated into a two-level Ising Hamiltonian governed by long-range coupling, characteristic of dipolar systems. Additionally, the applied magnetic field yields a term which does not commute with the Hamiltonian and, therefore, the composite system can be described by a transverse Ising model (TIM). The latter exhibits a quantum phase transition at zero temperature wherein the system transits from a ferromagnetic phase to a paramagnetic phase as the strength of the transverse field is increased.

The main feature of I was the discussion of the ubiquitous magnetic hyperfine interaction between the Ho nuclear moment and its own electronic spin, which makes its presence felt especially at lower temperatures. Since it is the low-temperature regime in which the quantum nature of the phase transition becomes important, it is expected that the hyperfine coupling would have a significant effect, on both the static and dynamic properties. This was demonstrated in I by detailed calculations in the mean-field theory of the phase diagram as well as the dynamic susceptibility. Now one of the most versatile tools for probing the hyperfine interaction is nuclear magnetic resonance (NMR). Since the main physics issue in $LiHoF_4$ is in fact the occurrence of the quantum critical point and the associated phase transition characteristics, it would indeed be interesting to use NMR as a probe for investigating further the quantum phase transition in this prototypical system. We explore this possibility by computing NMR line shapes in $LiHoF_4$, using the Ho nucleus as the probe, and hoping thereby to spur new experiments in this system. The ensuing analysis is an extension of the calculational method outlined in I.

In heavy rare-earth ions such as Ho^{3+} the dominant contribution to the hyperfine field at the nucleus comes from the $4f$ electrons, which then leads to a quantum ''entanglement'' of nuclear and electronic spins in the background of an underlying quantum phase transition. One additional feature, omnipresent in rare-earth NMR, is a quadrupolar interaction for the nuclear moments arising from the lack of sphericity in the distribution of the electronic charges around the nucleus.

The paper is organized as follows. In Sec. II, we describe the representative Hamiltonian of the model magnet for the study of NMR line shapes. The underlying mean-field theory is formulated in Sec. III, whereas the line shape calculation is presented in Sec. IV, with the aid of a stochastic model. In Sec. V we discuss an *ab initio* many-body treatment which provides justification for the stochastic method of Sec. IV. Finally, Sec. VI contains the computed spectra and their analysis.

II. HAMILTONIAN

The appropriateness of the TIM in conjunction with hyperfine interactions, for describing the static and dynamic properties of the dipolar coupled $LiHoF_4$, has been discussed in great detail in I. We represented holmium moments by Ising spins making use of the fact that at the low operating temperatures of $LiHoF_4$ wherein the system shows a perfect mean-field ferromagnetic transition at a temperature of 1.53 K, only the two lowest crystal-field-split levels are predominantly occupied. Thus the dipolar interaction between the holmium moments can be adequately described by an Ising Hamiltonian. Although the basic structure of the Hamiltonian remains unchanged in the present context, an important difference arises from the need to include the quadrupolar interaction in the Hamiltonian, especially for rare-earth alloys. While the quadrupolar interaction, which is at least two orders of magnitude smaller than the corresponding dipolar hyperfine interaction, does not significantly alter the static phase diagram and the dynamic susceptibility calculated in I, it substantially affects the NMR spectrum for the following reasons. A nucleus with a spin angular momentum I in a magnetic field yields $(2I+1)$ equally spaced values of the magnetic field quantum number M. An NMR experiment

normally excites transitions between adjacent levels, the selection rule being $\Delta M = \pm 1$. For a set of $(2I+1)$ evenly spaced levels, there would be just a single NMR frequency, but for the presence of quadrupolar interactions. Hence in rare-earth NMR, unlike most NMR, inclusion of the quadrupolar interaction is a must. Thus a good representation of $LiHoF_4$ is the TIM with hyperfine interactions of both the dipolar and the quadrupolar variety :

$$\mathcal{H}_s = -\sum_{i,j=1}^{N} J_{ij}\sigma_i^z\sigma_j^z - \sum_{i=1}^{N} aI_i^z\sigma_i^z + Q\sum_{i=1}^{N}[3(I_i^z)^2 - I_i^2] - \Omega\sum_{i=1}^{N}\sigma_i^x. \quad (1)$$

In Eq. (1), the interaction energy J_{ij} for the magnetic holmium moments, recalling its origin in dipolar coupling, is given by[2,3]

$$J_{ij} = g^2\mu^2[1-3\cos^2(\theta_{ij})]/r_{ij}^3, \quad (2)$$

where g is the gyromagnetic ratio, μ the Bohr magneton, and r_{ij} and θ_{ij} are, respectively, the magnitude and polar angle of the vector $(\overline{r_i} - \overline{r_j})$ connecting sites i and j. The angle θ_{ij} is distributed between 0 and π, causing the sign of J_{ij} to fluctuate between positive and negative. With competing interactions and the long-ranged nature of the dipolar interaction, it is not obvious that the ground state is ferromagnetic. However, it has been shown experimentally and theoretically that the ground-state ordering, which is determined by the lattice structure, is indeed ferromagnetic in the present instance.[4]

The second term in Eq. (1) represents the hyperfine interaction between the nuclear spin I_i^z and the electronic spin σ_i^z of Ho^{3+}. For $LiHoF_4$, the hyperfine coupling constant a has been tabulated from electron paramagnetic resonance (EPR) experiments to be 0.039 K.[6,7] Usually the hyperfine interaction is isotropic, but because of the inherent spin anisotropy along the z axis (c axis), the component of the g tensor along this direction is at least an order of magnitude larger than the transverse component. Thus the hyperfine interaction in Eq. (1) can be assumed to be diagonal. The validity of this approximation has been checked in I. The third term represents the interaction of the nuclear quadrupolar moment with the electric field gradient of the nucleus.[3,8]. While this term too can be isotropic, the z component provides the dominant contribution for reasons just cited. In Ho^{3+} the quadrupolar interaction is smaller than the dipolar hyperfine interaction by two orders of magnitude, yet it has a nontrivial influence on the NMR line shapes. This is because the operator σ_i^z in the dipolar hyperfine term can get relaxationally averaged to zero due to dynamics as well as heat bath coupling.

The last term in Eq. (1) induces tunneling effects by mixing the eigenstates corresponding to the σ_z operator. This introduces quantum dynamics into the system, making H_s the prototype Hamiltonian of a quantum magnet. In the experiments of Bitko *et al.*,[5] this is realized by the application of a magnetic field H_t perpendicular to the c axis. This field can cause an admixture of the crystal-field-split states, yielding in perturbation theory a spin Hamiltonian that depends on σ^x with a prefactor Ω which is quadratic in H_t.

III. MEAN-FIELD THEORY

As in I, in the mean-field approximation, the single-site Hamiltonian for Eq. (1) can be written as

$$\mathcal{H}_s = E_Q - (aI^z + H)\sigma^z - \Omega\sigma^x, \quad (3)$$

where we have substituted

$$E_Q = Q[3(I^z)^2 - I^2] \quad (4)$$

and

$$H = J(0)\langle\sigma^z\rangle, \quad (5)$$

with $J(0) = \Sigma_j J_{ij}$. The partition function is given by

$$Z = \mathrm{Tr}(e^{-\beta\mathcal{H}_s}) = \mathrm{Tr}\, e^{-\beta[E_Q - (aI^z+H)\sigma^z - \Omega\sigma^x]}. \quad (6)$$

The trace in Eq. (6) is over the electronic as well as the nuclear spin eigenstates. Labeling the eight nuclear eigenstates by $|M\rangle$, we have $I^z|M\rangle = M|M\rangle$, $M = -7/2, \ldots, 7/2$. Thus the partition function Z can now be written as

$$Z = \sum_{M=-7/2}^{7/2} e^{-\beta E_Q^M}\mathrm{Tr}\, e^{\beta[(aM+H)\sigma^z - \Omega\sigma^x]}, \quad (7)$$

where $E_Q^M = 3Q(M^2 - \frac{21}{4})$. The trace now is over the eigenstates of the electronic spin σ^z alone. Using the property of Pauli matrices, Eq. (7) can be simplified as

$$Z = \sum_{M=-7/2}^{7/2} e^{-\beta E_Q^M}\cosh[\beta h(M)], \quad (8)$$

where

$$h(M) = \sqrt{(aM+H)^2 + \Omega^2}. \quad (9)$$

Following I, the self-consistent relation for the z component of magnetization $m^z = \langle\sigma^z\rangle$ is given by

$$m^z = \frac{\sum_M e^{-\beta E_Q^M}\left(\frac{aM + J(0)m^z}{h(M)}\right)\sinh[\beta h(M)]}{\sum_M e^{-\beta E_Q^M}\cosh[\beta h(M)]}. \quad (10)$$

The phase diagram of the system in the Ω-T plane in the presence of a dipolar hyperfine interaction was presented in I. We have checked that the phase diagram is negligibly altered if the quadrupolar interaction term of strength $0.01a$ is included in addition to the dipolar hyperfine interaction.

The Hamiltonian of Eq. (3) describes the reversible dynamics of the system. Since the subject of investigation is NMR line shapes which are affected by the spin-spin and spin-lattice relaxations, it is necessary to introduce irreversible effects leading to dissipative dynamics of the system. As in I, to include these effects we couple the system described by Eq. (3) to the surrounding heat bath:

$$\mathcal{H}_o = \mathcal{H}_S + \mathcal{H}_I + \mathcal{H}_B, \quad (11)$$

where $\mathcal{H}_I$ describes the interaction between the spin system and the heat bath. In order to obtain an appropriate expression for $\mathcal{H}_I$, it is convenient to first rotate in the angular momentum space of $\overline{\sigma}$ about the y axis (in a clockwise direction) by an angle $\theta = \arctan(\Omega/H_0)$. This is achieved by the rotation operator

$$U_Y^R = e^{-i\theta\sigma^y}, \tag{12}$$

where

$$H_0 = \sqrt{H^2+\Omega^2}. \tag{13}$$

In the rotated frame, the total Hamiltonian is

$$\tilde{\mathcal{H}}_0 = \tilde{\mathcal{H}}_S + \tilde{\mathcal{H}}_I + \mathcal{H}_B, \tag{14}$$

while the subsystem Hamiltonian $\tilde{\mathcal{H}}_S$, which is now diagonal, is given by

$$\tilde{\mathcal{H}}_S = E_Q - \frac{aI^z}{H_0}(H\sigma^Z + \Omega\sigma^x) - H_0\sigma^z. \tag{15}$$

It may be noted that the transformation introduced above is different from the one employed in I. The advantage of the present scheme is that the NMR transition operator I^x remains unchanged by the rotation, although the hyperfine coupling becomes off diagonal in the electronic system.

In the following section we present a stochastic approach to the calculation of the resonance line shape which is physical and takes explicit cognizance of the stochastic forces in the system. In this stochastic picture, the hyperfine coupled nucleus-electron system is envisaged to be embedded in a random environment, the randomness being the result of spin-lattice relaxational processes which make the electron-spin feel time-fluctuating stochastic fields. Thus, following Clauser and Blume,[9] we imagine that the subsystem Hamiltonian given by Eq. (3) is subject to pulses, the distribution of which follows a Poisson process. The strategy adopted here is similar to the one employed in an NMR calculation in proton glasses.[10]

IV. RESONANCE LINE SHAPE

The NMR line shape is given by

$$J(\omega) = \frac{1}{\pi} \lim_{s \to -i\omega+\delta} \mathrm{Re}[\tilde{C}(s)], \tag{16}$$

where $\tilde{C}(s)$ is the Laplace transform of the correlation function defined as

$$C(t) = \langle I^x(0) I^x(t) \rangle_{eq}. \tag{17}$$

Here the angular brackets denote the appropriate quantum and statistical average. The quantity s is related to the applied frequency ω and δ is a small real-valued parameter which not only ensures convergence of Laplace transforms but takes into account possible instrumental broadening. We would like to point out here that in I, we calculated the electronic spin correlation function $\langle \sigma^z(0)\sigma^z(t)\rangle$, necessary for computing the dynamic susceptibility. In the present context, since we are interested in studying the relaxational effects in the system on the *nuclear* spin via an NMR experiment, the appropriate quantity to calculate must involve the off-diagonal operator I^x which causes resonance transitions in the Hilbert space of the I spins.

The Clauser-Blume solution for $\tilde{C}(s)$ is given by

$$\tilde{C}(s) = \sum_{MM'} |\langle M|I^x|M'\rangle|^2 (M'M|\overline{[\tilde{U}(s)]_{av}}|M'M), \tag{18}$$

where the over bar on top of the time-development operator indicates an average over the ''electronic'' states:

$$\overline{[\tilde{U}(s)]_{av}} = \sum_{\mu,\nu} p_\nu (\nu\nu|[\tilde{U}(s)]_{av}|\mu\mu), \tag{19}$$

p_ν being the Boltzmann factor associated with the electronic state $|\nu\rangle$,

$$p_\nu = e^{\beta H_0 \nu}[2\cosh(\beta H_0)]^{-1}, \tag{20}$$

whereas $[\cdots]_{av}$ implies a stochastic average. Now, detailed balance of transitions require that for a spin-half system,[8]

$$\bar{\tilde{U}}(s) = \frac{\overline{\tilde{U}^0}(s+\lambda)}{1-\lambda\overline{\tilde{U}^0}(s+\lambda)}, \tag{21}$$

where λ is a phenomenologically introduced relaxation rate and

$$\overline{\tilde{U}^0}(s+\lambda) = \sum_{\nu\mu} p_\nu (\nu\nu|[s+\lambda-i\mathcal{L}_S]^{-1}|\mu\mu), \tag{22}$$

$\mathcal{L}_S$ being the Liouville operator associated with $\tilde{\mathcal{H}}_S$ in Eq. (15). Since the latter is diagonal among the angular momentum states of the nucleus, because it contains only I^z, we can further write

$$\tilde{C}(s) = \sum_{MM'} |\langle M|I^x|M'\rangle|^2 \frac{\tilde{G}_{MM'}(s+\lambda)}{1-\lambda\tilde{G}_{MM'}(s+\lambda)}, \tag{23}$$

where

$$\tilde{G}_{MM'}(s+\lambda) = (M'M|\overline{\tilde{U}^0}(s+\lambda)|M'M). \tag{24}$$

In order to evaluate $\tilde{G}_{MM'}(s+\lambda)$ from Eq. (24) we have to first rewrite the expression in Eq. (22) as an integral over time and then use the definition for the exponential of a Liouville operator, thus obtaining

$$\tilde{G}_{MM'}(s+\lambda)=\int_0^\infty dt e^{-(s+\lambda)t}\sum_{\mu,\nu} p_\nu \times\langle \nu M'|e^{i\tilde{\mathcal{H}}_S t}|\mu M'\rangle\langle \mu M|e^{-i\tilde{\mathcal{H}}_S t}|\nu M\rangle. \tag{25}$$

Our next step is to employ the fact that $\tilde{\mathcal{H}}_S$ is diagonal in the I^z representation and also use the following property of the Pauli matrices[11]:

$$\exp(it\overline{\sigma}\cdot\overline{h})=\cos(ht)\mathbf{1}+i\sin(ht)\left(\frac{\overline{\sigma}\cdot\overline{h}}{h}\right). \tag{26}$$

After some straightforward algebra we obtain

$$\begin{aligned}\tilde{G}_{MM'}(s+\lambda)=&\frac{1}{4}[(s+\lambda)-i(E_Q^{M'}-E_Q^M)-i(h+h')]^{-1}[1-A_{MM'}+B_{MM'}\tanh(\beta H_0)]\\ &\times\frac{1}{4}[(s+\lambda)-i(E_Q^{M'}-E_Q^M)+i(h+h')]^{-1}[1-A_{MM'}-B_{MM'}\tanh(\beta H_0)]\\ &\times\frac{1}{4}[(s+\lambda)-i(E_Q^{M'}-E_Q^M)-i(h-h')]^{-1}[1+A_{MM'}+C_{MM'}\tanh(\beta H_0)]\\ &\times\frac{1}{4}[(s+\lambda)-i(E_Q^{M'}-E_Q^M)+i(h-h')]^{-1}[1+A_{MM'}-C_{MM'}\tanh(\beta H_0)],\end{aligned} \tag{27}$$

where

$$h=\left[\left(H_0+\frac{aH}{H_0}M\right)^2+\frac{a^2\Omega^2}{H_0^2}\right]^{1/2}, \tag{28}$$

$$h'=\left[\left(H_0+\frac{aH}{H_0}M'\right)^2+\frac{a^2\Omega^2}{H_0^2}\right]^{1/2}, \tag{29}$$

$$A_{MM'}=\frac{1}{hh'}\left[\left(H_0+\frac{aH}{H_0}M\right)\left(H_0+\frac{aH}{H_0}M'\right)+\frac{a^2\Omega^2}{H_0^2}\right], \tag{30}$$

$$B_{MM'}=\frac{1}{hh'}\left[h'\left(H_0+\frac{aH}{H_0}M\right)-h\left(H_0+\frac{aH}{H_0}M'\right)\right], \tag{31}$$

$$C_{MM'}=\frac{1}{hh'}\left[h'\left(H_0+\frac{aH}{H_0}M\right)+h\left(H_0+\frac{aH}{H_0}M'\right)\right]. \tag{32}$$

With the expression for $\tilde{G}_{MM'}(s+\lambda)$ at hand, the NMR line shape can be evaluated from Eq. (16), in which [cf. Eq. (23)]

$$\tilde{C}(s)=\frac{1}{4}\sum_M\left[(I-M)(I+M+1)\frac{\tilde{G}_{M,M+1}(s+\lambda)}{1-\lambda\tilde{G}_{M,M+1}(s+\lambda)}+(I+M)(I-M+1)\frac{\tilde{G}_{M,M-1}(s+\lambda)}{1-\lambda\tilde{G}_{M,M-1}(s+\lambda)}\right]. \tag{33}$$

V. RESOLVENT EXPANSION

In the discussion in Sec. IV the effect of the fluctuating environment was tacitly taken into account via stochastic forces. In order to incorporate the effects of the heat bath and its coupling to the subsystem more explicitly we will have to go back to the full Hamiltonian of Eq. (14) and provide a many-body treatment. The advantage of such an *ab initio* approach is not only to lend justification to the stochastic method but also to give proper meaning to the phenomenological parameters such as the relaxation rate λ. Before we do that, it is necessary to model the interaction Hamiltonian in the rotated frame, viz., $\tilde{\mathcal{H}}_I$, which we choose to have the following form:

$$\tilde{\mathcal{H}}_I=\frac{1}{2}\sum_q g_q\{\sigma^z(b_q+b_q^\dagger)+(b_q\sigma_+ +b_q^\dagger\sigma_-)\}, \tag{34}$$

where b_q and $b_q^\dagger$ are phonon annihilation and creation operators for the qth phonon mode while $\sigma_\pm$ are the ladder operators for the electron spin. The coupling constant g_q is taken to be arbitrary.

The interaction Hamiltonian in Eq. (34) is a standard prescription for treating spin lattice relaxation. Further, since in the rotated space the electronic part of the subsystem Hamiltonian is diagonal in the σ^z representation (barring the hyperfine coupling), the interaction term causes spin flips via the ladder operators. The latter processes lead to Glauber-like kinetics of the underlying Ising model.[12]

It may be noted that the central quantity we need for the line shape calculation [cf. Eq. (18)] is the Laplace transform of the time-development operator $[\tilde{U}(s)]_{av}$, where $[\cdots]_{av}$ now indicates the explicit average over the density matrix

associated with the bath Hamiltonian $\mathcal{H}_B$. A convenient form of the latter is achieved by writing a resolvent expansion of $[\tilde{U}(s)]_{av}$ in which the interaction term $\tilde{\mathcal{H}}_I$ is treated perturbatively.[8] Thus we can use the following general expression for $[\tilde{U}(s)]_{av}$:

$$[\tilde{U}(s)]_{av}=[s-i\mathcal{L}_S+\tilde{\Sigma}(s)]^{-1}, \tag{35}$$

where $\mathcal{L}_S$ is the Liouville operator associated with the spin Hamiltonian $\mathcal{H}_S$, defined in Eq. (3), and $\tilde{\Sigma}(s)$ is the so-called relaxation matrix, to be specified below. While it is possible to evaluate $\tilde{\Sigma}(s)$ to arbitrary orders in perturbation theory, it suffices for the purpose of obtaining Markovian dynamics to use an expansion upto second order in $\tilde{\mathcal{H}}_I$, which yields[8]

$$\tilde{\Sigma}(s)=\left[\mathcal{L}_I\frac{1}{s-i\mathcal{L}_S-i\mathcal{L}_B}\mathcal{L}_I\right]_{av}. \tag{36}$$

The next step is the evaluation of the relaxation matrix $\tilde{\Sigma}(s)$. We treat the heat bath in the Markovian approximation, i.e., neglect the frequency dependence of the relaxation matrix. Hence it is possible to write

$$\tilde{\Sigma}(s)\approx\tilde{\Sigma}(0)=\int_0^\infty dt[\mathcal{L}_I(e^{i(\mathcal{L}_S+\mathcal{L}_B)t})\mathcal{L}_I]_{av}. \tag{37}$$

Using the properties of the Liouville operator[8] and after some algebra, in which we ignore the (tiny) influence of the hyperfine interaction on the relaxation behavior, we can write the matrix elements of $\tilde{\Sigma}(s)$ in the angular momentum space of the electronic spin as

$$\begin{aligned}(\mu\nu|\tilde{\Sigma}(0)|\mu'\nu')&=\sum_q\frac{g_q^2}{4}\int_0^\infty dt\Bigg\{\delta_{\mu\mu'}\delta_{\nu\nu'}\Bigg[\sum_{\mu_1}e^{-iH_0t(\mu_1-\nu)}A\\&+\sum_{\nu_1}e^{-iH_0t(\mu-\nu_1)}B\Bigg]-C-D\Bigg\},\end{aligned} \tag{38}$$

where we have made the following substitutions:

$$\begin{aligned}A&=\langle\mu|\sigma_+|\mu_1\rangle\langle\mu_1|\sigma_-|\mu\rangle\langle\langle b_q(0)b_q^\dagger(t)\rangle\rangle\\&\quad+\langle\mu|\sigma_-|\mu_1\rangle\langle\mu_1|\sigma_+|\mu\rangle\langle\langle b_q^\dagger(0)b_q(t)\rangle\rangle,\\B&=\langle\nu'|\sigma_+|\nu_1\rangle\langle\nu_1|\sigma_-|\nu\rangle\langle\langle b_q(t)b_q^\dagger(0)\rangle\rangle\\&\quad+\langle\nu'|\sigma_-|\nu_1\rangle\langle\nu_1|\sigma_+|\nu\rangle\langle\langle b_q^\dagger(t)b_q(0)\rangle\rangle,\\C&=\langle\mu|\sigma_+|\mu'\rangle\langle\nu'|\sigma_-|\nu\rangle[e^{-iH_0t(\mu-\nu')}\\&\quad\times\langle\langle b_q(t)b_q^\dagger(0)\rangle\rangle+e^{-iH_0t(\mu'-\nu)}\langle\langle b_q(0)b_q^\dagger(t)\rangle\rangle],\\D&=\langle\mu|\sigma_-|\mu'\rangle\langle\nu'|\sigma_+|\nu\rangle[e^{-iH_0t(\mu-\nu')}\\&\quad\times\langle\langle b_q^\dagger(t)b_q(0)\rangle\rangle+e^{-iH_0t(\mu'-\nu)}\langle\langle b_q^\dagger(0)b_q(t)\rangle\rangle].\end{aligned}$$

In Eq. (39), $\langle\langle\cdots\rangle\rangle$ denotes bath-averaged phonon correlation functions.

A representative element of the $\tilde{\Sigma}(0)$ matrix can be calculated as

$$\begin{aligned}&(+,+|\tilde{\Sigma}(0)|+,+)\\&\quad=\sum_q g_q^2\int_0^{+\infty}dt[e^{2iH_0t}\langle\langle b_q(0)b_q^\dagger(t)\rangle\rangle\\&\qquad+e^{-2iH_0t}\langle\langle b_q(t)b_q^\dagger(0)\rangle\rangle],\end{aligned} \tag{39}$$

which upon using the time-symmetry property of the phonon correlation functions can be rewritten as

$$\begin{aligned}&(+,+|\tilde{\Sigma}(0)|+,+)\\&\quad=\int_{-\infty}^{+\infty}dte^{-2iH_0t}\sum_q g_q^2\langle\langle b_q(t)b_q^\dagger(0)\rangle\rangle.\end{aligned} \tag{40}$$

Similarly,

$$\begin{aligned}&(-,-|\tilde{\Sigma}(0)|-,-)\\&\quad=\int_{-\infty}^{+\infty}dte^{2iH_0t}\sum_q g_q^2\langle\langle b_q^\dagger(t)b_q(0)\rangle\rangle.\end{aligned} \tag{41}$$

If the heat bath Hamiltonian $\mathcal{H}_B$ is taken to describe a free phonon system, it is easy to write down the phonon correlation functions. For instance,[13]

$$\langle\langle b_q^\dagger(t)b_q(0)\rangle\rangle=\coth\left(\frac{1}{2}\hbar\beta\omega_q\right)\cos(\omega_qt)+i\sin(\omega_qt). \tag{42}$$

However, if the thermal energy is much larger than the energy of the highest phonon mode (of the order of the Debye frequency), as is indeed the case in the Markovian limit of the heat bath, the imaginary component of the correlation function, as given above, can be neglected. Thus we assume that

$$\begin{aligned}\sum_q g_q^2\langle\langle b_q(t)b_q^\dagger(0)\rangle\rangle&\approx\sum_q g_q^2\langle\langle b_q^\dagger(t)b_q(0)\rangle\rangle\\&\approx\sum_q g_q^2\langle\langle b_q(0)b_q^\dagger(t)\rangle\rangle\\&\approx\sum_q g_q^2\langle\langle b_q^\dagger(0)b_q(t)\rangle\rangle\equiv\frac{1}{4}\Phi(t),\end{aligned} \tag{43}$$

where $\Phi(t)$ is real and is a symmetric function of t.

Further, we can establish the following Kubo relation leading to a detailed balance of transitions:

$$(+,+|\tilde{\Sigma}(0)|+,+)=e^{-2\beta H_0}(-,-|\tilde{\Sigma}(0)|-,-). \tag{44}$$

Hence, in the Markovian approximation,

$$(+,+|\tilde{\Sigma}(0)|+,+)=-(+,+|\tilde{\Sigma}(0)|-,-)=\lambda p_-,$$

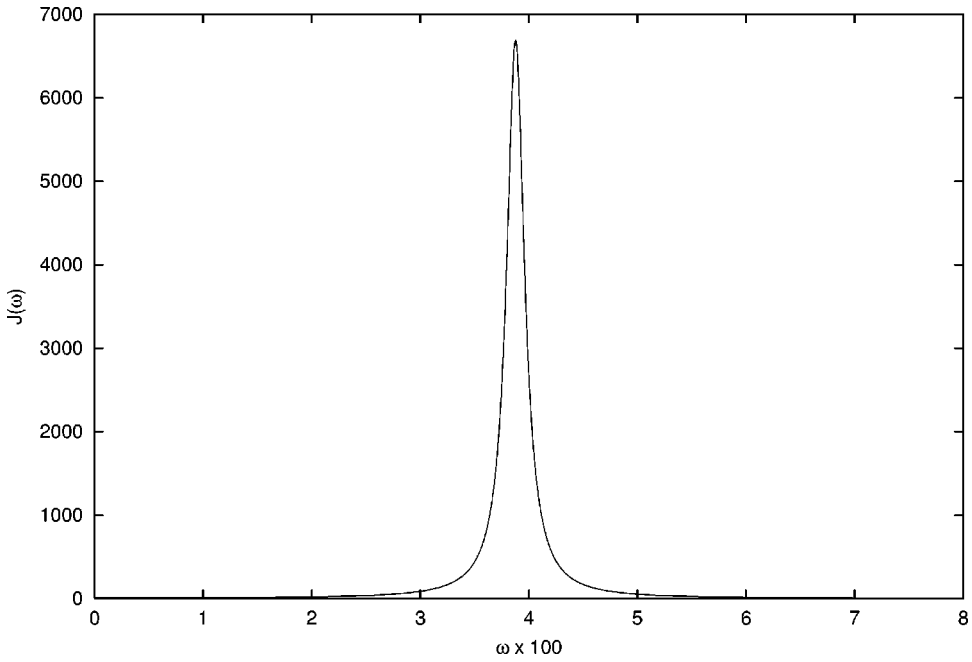

FIG. 1. Computed $J(\omega)$ vs ω in the absence of a quadrupolar interaction. T and R have been selected to be 0.1 K and 0.1, respectively.

$$(-,-|\tilde{\Sigma}(0)|-,-)=-(-,-|\tilde{\Sigma}(0)|+,+)=\lambda p_+, \tag{45}$$

where the Boltzman factors $p_\pm$ are given by Eq. (20) and the relaxation rate λ is

$$\lambda=\int_0^\infty dt\Phi(t). \tag{46}$$

Therefore, the relaxation matrix $\tilde{\Sigma}(0)$ can be expressed as

$$\tilde{\Sigma}(0)=\lambda(\mathbf{1}-\mathcal{T}), \tag{47}$$

where **1** is the unit matrix and $\mathcal{T}$ the "transition" matrix with elements given by

$$(\mu\nu|\mathcal{T}|\mu'\nu')=p_{\mu'}\delta_{\mu\nu}\delta_{\mu'\nu'}. \tag{48}$$

Combining Eq. (35) with Eq. (47), we have

$$[\tilde{U}(s)]_{av}=[(s+\lambda)-i\mathcal{L}_S-\lambda\mathcal{T}]^{-1}. \tag{49}$$

Recall from Eq. (19) that what we need in the line shape

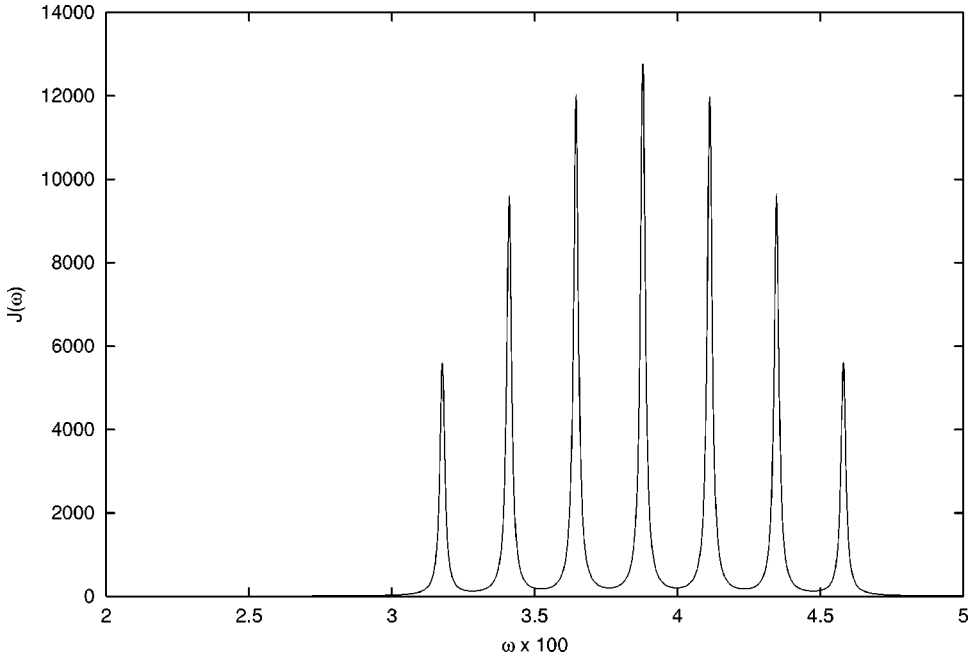

FIG. 2. $J(\omega)$ vs ω in the presence of a tiny quadrupolar interaction term for $R=0.1$.

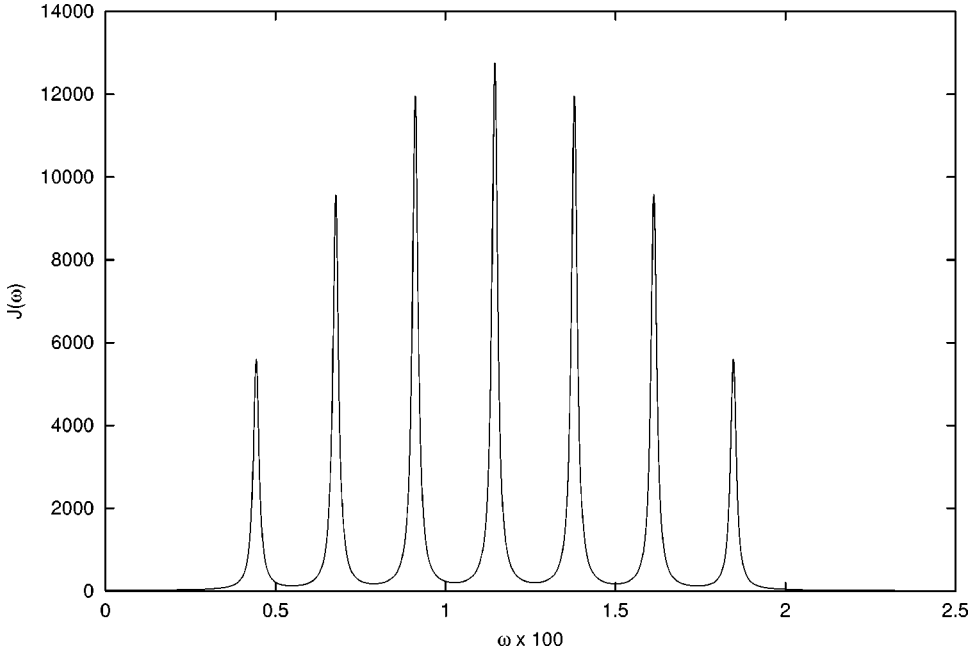

FIG. 3. $J(\omega)$ vs ω for $R=0.95$, close to the quantum critical point.

calculation is a further averaging of Eq. (49) over electronic states. Developing Eq. (49) then as a Dyson series, we can write Eq. (19) as

$$\overline{[\tilde{U}(s)]_{av}}=\overline{\tilde{U}^0(s+\lambda)} + \lambda\sum_{\mu\nu} p_\nu \left(\nu\nu \left| \frac{1}{s+\lambda-i\mathcal{L}_S} \mathcal{T}[\tilde{U}(s)]_{av} \right| \mu\mu \right), \tag{50}$$

which, upon employing the closure property of states as

$$\sum_{\mu'\nu'} |\nu'\mu')(\nu'\mu'| = \mathbf{1} \tag{51}$$

and regrouping of terms, yields Eq. (21) of Sec. IV.

From this point onwards then the computation of the NMR line shape proceeds exactly as in Sec. IV, culminating in Eq. (33). We may therefore conclude this section by reiterating that the *ab initio* resolvent expansion treatment discussed here not only complements the stochastic model calculation of the previous section but also provides a more detailed rationale behind some of the basic assumptions involved in the stochastic model. The heat-bath-induced fluctuation effects are embodied in a parameter λ, the so-called

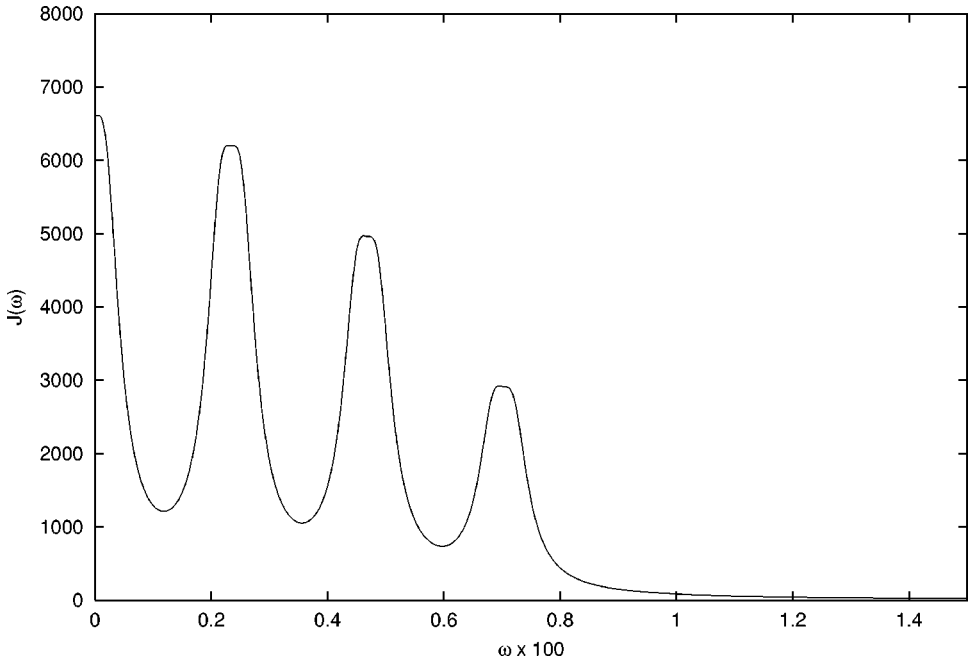

FIG. 4. $J(\omega)$ vs ω at the quantum critical point $R=1.0$. The spectrum changes from a seven-line to a four-line one at the quantum critical point. See text of Sec. VI.

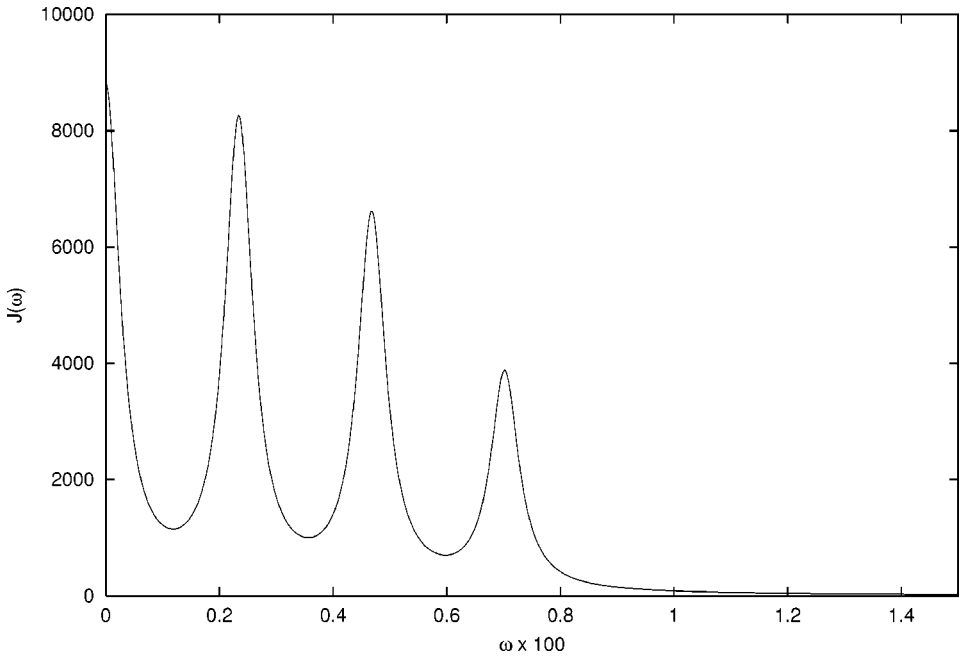

FIG. 5. $J(\omega)$ vs ω above the quantum critical point for $R=2.0$.

relaxation rate, the meaning of which is also amplified through the present discussion [cf. Eq. (46)].

VI. COMPUTED NMR SPECTRA AND DISCUSSION

There are four parameters which need to be defined for the computation of NMR spectra. The hyperfine constant a is taken from the literature as 0.039 K. Since the quadrupolar interaction is about two orders of magnitude less than a, we select $Q=0.01a$. The parameter δ has been given a small value of 0.0001 K. The relaxation rate λ is actually the only free parameter. For comparison with experimental data it is convenient to parametrize λ, although it is possible to calculate it from first principles using the results of Sec. V. Such a calculation would, however, require a detailed modeling of the bath and assumptions about the nature of the phonons, e.g., acoustic or optic. At the level of the NMR line shape we feel it is reasonable to simply use λ as a fitting parameter. Thus we select λ to be 1 K. Small values of λ resulted in extremely slow relaxation as opposed to the fast relaxation of larger values of λ. The results presented are robust over at least a decade of λ values. Since hyperfine interactions are effective only at low temperatures, we have selected $T=0.1$ K (refer to Fig 1 in I). We define R to be the ratio of the transverse field $\Omega(T)$ to the critical transverse field $\Omega_c(T)$ at the specific value of temperature T.

We first study the effect of the quadrupolar interaction on the NMR spectrum. In Fig. 1, we plot $J(\omega)$ vs ω [Eq. (33)] for $R=0.1$ and $Q=0.0$. As mentioned earlier in Sec. I, in the absence of quadrupolar interactions, the $(2I+1)$ equally spaced hyperfine levels yield a single NMR frequency as observed from Fig. 1. Since the abscissa in Fig. 1 is taken as $\omega\times 100$, it is clear why this frequency is valued near $3.9(=0.039\times 100)$. This is because when the temperature T is as low as 0.1 K and the transverse field is ''small,'' the electronic spins have almost perfect ferromagnetic ordering. Therefore the term σ^z in the hyperfine interaction, $aI^z\sigma^z$, can be replaced by unity, and the NMR frequency equals $aM-a(M-1)=a$.

The inclusion of a small quadrupolar interaction $Q=0.01a$ results in eight unequally distributed energy levels. Since the selection rule is $\Delta M=\pm 1$, we observe a seven-peak structure in Fig. 2. The peak to the extreme left corresponds to the $-\frac{7}{2}\rightarrow-\frac{5}{2}$ transition while the peak to the extreme right corresponds to the $\frac{5}{2}\rightarrow\frac{7}{2}$ transitions. The respective intensities are governed by the matrix elements of the transition operator I^x.

In Figs. 3, 4, and 5, we show the effect of the transverse field on the NMR spectrum. These correspond to $R=0.95$, 1.0, and 2.0, respectively. The transverse field, like temperature, is a disordering field. Hence we see that as Ω increases, the system moves from the ferromagnetic to the paramagnetic phase. This behavior is accompanied by rapid fluctuation of the electronic component of the spin in the hyperfine interaction, even though the temperature is low. The point is that the temperature controls the heat-bath-induced relaxation effects whereas it is the transverse field that triggers the motion of the electronic spin due to quantum dynamics. Thus, for large values of the transverse field R, the hyperfine interaction is ''motionally averaged out,'' leaving behind merely the quadrupolar interaction [cf. Eq. (3) and Eq. (15)]. This phenomenon is evident in Fig. 5: the spectrum collapses into a four-line one corresponding to the eigenvalues of E_Q [cf. Eq. (4)], each of which is doubly degenerate, yielding lines located at 0, $6Q$, $12Q$, and $18Q$. In between, for intermediate values of R (see Figs 3 and 4), the lines undergo a ''lifetime broadening'' due to tunneling caused by the increasing value of the transverse field.

We would, however, like to point out that our mean-field theory is expected to break down very close to the quantum critical point wherein strong correlation effects of both classical and quantum nature, neglected in our treatment, will become important. Because of the limitation of the theory,

we have restricted the line shape computation to temperatures which in energy scales are higher than hyperfine interactions. It will be very useful to employ quantum Monte Carlo or similar methods to explore the region near $T=0$ K and ascertain the role of the hyperfine coupling in that regime of quantum phase transition. Studies along these lines are in progress.

It is pertinent to mention once again that all the figures, Figs. 1–5, have been drawn for a fixed value of the relaxation rate λ which has been kept sufficiently low. The idea was to suppress thermal fluctuations but to emphasize the importance of quantal fluctuations caused by the transverse field. For the same very reason, the temperature has been kept small (but higher than the hyperfine interaction) such that quantum phase transition effects are prominent. Indeed it is observed that the hyperfine coupling including the quadrupolar interaction can be effectively used as a marker for studying the quantum phase transition in general and the quantum critical point in particular. In that sense NMR can be employed as a very useful tool and one that is complementary to ac susceptibility in a quantum magnet such as $LiHoF_4$. It is hoped that these observations would spur further experimental work in this system.

ACKNOWLEDGMENTS

V.B. acknowledges useful discussions with R. G. Mendiratta and support of C.S.I.R. Grant No. 03(0929)/01/EMR-II.

*Electronic address: varsha@physics.iitd.ernet.in
†Electronic address: sdgupta@bose.res.in

[1] V. Banerjee and S. Dattagupta, Phys. Rev. B **64**, 024427 (2001).
[2] C.P. Slichter, *Principles of Magnetic Resonance* (Harper and Row, New York, 1963).
[3] A. Abragam, *The Theory of Nuclear Magnetism* (Oxford University Press, London, 1961).
[4] J.M. Luttinger and L. Tisza, Phys. Rev. **70**, 954 (1946).
[5] D. Bitko, T.F. Rosenbaum, and G. Aeppli, Phys. Rev. Lett. **77**, 940 (1996).
[6] G. Mennenga, L.J. de Jongh, and W.J. Huiskamp, J. Magn. Magn. Mater. **44**, 59 (1984).
[7] J. Megarino, J. Tuchendler, P. Beauvillian, and I. Laursen, Phys. Rev. B **21**, 18 (1980).
[8] S. Dattagupta, *Relaxation Phenomena in Condensed Matter Physics* (Academic, Orlando, FL, 1987).
[9] M.J. Clauser and M. Blume, Phys. Rev. B **3**, 583 (1971).
[10] S. Dattagupta, B. Tadic, R. Pirc, and R. Blinc, Phys. Rev. B **44**, 4387 (1991).
[11] See, for instance, A. Messiah, *Quantum Mechanics* (North-Holland, Amsterdam, 1965), Vol. II, Chap. XIII.
[12] K. Kawasaki, in *Phase Transitions and Critical Phenomena* Vol. 2, edited by C. Domb and M. S. Green (Academic, London, 1972).
[13] See, for instance, T. Qureshi and S. Dattagupta, Pramana **35**, 579 (1990).